

Breast Cancer Detection Using Microwaves by Changing the Electrical Properties of Tissues

Azhar Albaaj¹

¹Electrical Engineering Department, Amirkabir University of Technology (Tehran Polytechnic),
Tehran, Iran

Email: azhar.albaaj@aut.ac.ir

Yaser Norouzi^{*,1}

¹Electrical Engineering Department, Amirkabir University of Technology (Tehran Polytechnic),
Tehran, Iran

Email: y.norouzi@aut.ac.ir

Gholamreza Moradi¹

¹Electrical Engineering Department, Amirkabir University of Technology (Tehran Polytechnic),
Tehran, Iran

Email: ghmoradi@aut.ac.ir

*Corresponding Author: Yaser Norouzi (y.norouzi@aut.ac.ir)

Abstract

Worldwide, breast cancer is one of the leading causes of death among women. However, effective treatments are available for this type of cancer if diagnosed early. The difference in electrical properties between normal and malignant breasts is the basis for detecting the tumor and its location; in this article, the tumor is detected based on the change in conductivity and permittivity values in tissues between the two cases if a tumor is present and if it is not. In this paper, CADFEKO 2018 was used to simulate a design composed of hemispherical breast tissue and two dipole antennas, one of which transmits and the other receives a signal. There is a difference between the results of a breast design that contains a tumor and a design that does not have a tumor, as shown by preliminary simulations and the results of the designs themselves. Thus, by analysing these outcomes and simulation-generated signals, we can determine whether a tumor exists or not.

Keywords: Breast Cancer Detection; Conductivity; Permittivity; Reflection Coefficient; Transmission Coefficient.

Tob Regul Sci. TM 2022;8(1): 2921-2931

DOI: doi.org/10.18001/TRS.8.1.221

1. Introduction

According to the American Cancer Society, breast cancer is the most common malignancy diagnosed in women. In the United States, approximately 287,850 new breast cancer cases are expected to be identified in 2022, with 43,250 people expected to die from the disease [1]. Breast

cancer screening methods are designed primarily to detect the disease before symptoms emerge[2]. Current breast cancer detection technologies, such as mammography and MRI, have several limitations, prompting the development of a new screening method known as microwave imaging. Because of the differences in electrical properties of benign, malignant, and healthy tissues and the use of non-ionising frequencies, microwave imaging is a viable alternative for detecting breast cancer [3, 4]. One of the newest methods for early detection of breast cancer is microwave imaging. Because both ionising radiation and breast compression are avoided, microwave imaging is a viable screening approach. It is also less expensive and can identify minimal cancers [3]. The approach is based on the fact that cancerous and benign tissues have different dielectric characteristics. Studies of human tissue dielectric properties in the microwave frequency range [5] demonstrate that the contrast between malignant and benign tissue reaches ten times in dielectric permittivity and conductivity.

For ease of modelling and imaging, a basic breast model is created in the CST microwave studio; it is a hemisphere with a radius of 50 mm, centred at (0, 0, 0) mm, and contains only breast tissue, with no skin layer, glandular masses and blood vessels. Four horn antennas evenly spaced around the breast transmit and receive microwave signals [6]; in this scenario, antenna 1 serves as the transmitter, while antennas 2 through 4 serve as receivers. The transmitted signal is a 5GHz bandwidth Gaussian pulse. The transition solver in the Computer Simulation Technology (CST) Microwave Studio is used to simulate the model, tuned for a 50dB accuracy[7]. The model logs the responses to the transmitted pulse from antenna 1 at the ports of antennas 2–4. These responses reflect the status of the breast in the absence of a tumor. The model is then tweaked to add a 2mm radius spherical tumor within the breast tissue, centred at (10, 10, 10) mm. The model is re-simulated, and the resulting data is recorded. The initial step in signal processing is to extract the tumour response from the raw measured data. This can be accomplished by subtracting the data from the breast without tumor from the data from the breast with tumor. This finding confirms that the delay-and-sum algorithm can identify breast cancer if a sufficiently precise time delay is produced to impart the appropriate shift on received signals[8].

A final set-up worthy of discussion is that presented in [9]. Using EM (electromagnetic software) FEKO, wideband and narrowband arrays were built, simulated, and optimised for high (44%), medium (33%), and low (7%) bandwidths, respectively. The breast model (phantom) is then illuminated with these arrays, and the received backscattered signals are acquired in the near field for each case. Following that, the frequency domain Microwave Imaging through Space-Time (MIST) beamforming technique is applied to these near field backscattered monostatic frequency response data for image reconstruction of the breast model [10]. They represent the breast in its simplest form (breast fat and tumor) as proof of the concept for employing the developed MISF imaging algorithm. In CADFEKO, a 3D model of a breast with an embedded tumor was created with a hemispherical breast tissue radius of 60 mm and spherical tumor sizes of 5 and 10 mm. This precise tumor size is that breast cancer can be cured if identified at a size of 5-10mm. The full-wave simulation software FEKO contains a built-in capability that allows Debye relaxation for

3D breast modelling. As previously stated, the dielectric characteristics of breast fat tissue and tumors fluctuate with frequency, as previously stated [11]. The dielectric relaxation response of the material at microwave frequencies is known as the Debye relaxation. It is a dielectric characteristics modelling technique that is frequency-dependent. The significant disparity in scattered energy is due to the large differential in dielectric characteristics between breast fat and tumor[12].

In this study, CADFEKO 2018 simulates hemispherical breast tissue using two dipole antennas, one transmits, and the other receives a signal. Simulations revealed that the effects of a breast design with a tumor differed from those of a design without a tumor. The tumor is detected based on the difference in conductivity and permittivity in the tissues between the two cases with and without the presence of the tumor.

The remainder of this work is structured as follows: The electrical properties of breast tissue are presented in Section II. Section III addresses the design of the breast phantoms. Section IV explains the simulation and results, and finally, Section V concludes the paper.

2. Electrical Properties of Breast Tissue.

Breast tissue is characterised by two critical electrical properties, the relative permittivity, ϵ_r and the conductivity, σ . Extensive research has determined a significant contrast between the values of these properties for healthy and malignant breast tissue, particularly in the microwave frequency range. However, identifying the exact relative permittivity or conductivity of a particular tissue type at a specific frequency is difficult since intrinsic variations in the tissue can be high.

The study concluded that there could be a 10:1 difference in insulating properties between cancerous and adipose tissues. However, the cancerous and glandular tissue difference is only about 10% [13]. The variation in dielectric properties is negligible due to other factors such as sample temperature, patient age, and time between ablation and measurements[14].

The scattered field occurs when the electrical parameters of the object to be imaged, such as a cancerous tumor, differ from the surrounding medium, such as tissue. Tissue electrical properties, such as electrical conductivity and relative permittivity, play an essential role in tumor diagnosis and detection because different tissues absorb different amounts of microwaves depending on their electrical properties[15].

Permittivity and conductivity can be calculated using the equations [16]:

$$\epsilon_r = 1.71 * f^{-1.13} + \frac{\epsilon_s^{-4}}{1 + \left(\frac{f}{25}\right)^2} \quad (1)$$

where, ϵ_s is the relative permittivity of the static, and f is the frequency (GHz).

$$\sigma = 1.35 * f^{0.13} * \sigma_{0.1} + \frac{0.0222 * (\epsilon_s - 4) * f^2}{1 + \left(\frac{f}{25}\right)^2} \quad (2)$$

According to the above equations, there is a relationship between electrical properties and frequency.

3. Design of the Breast Phantoms

If a signal with high bandwidth, most of the frequencies are absorbed in the body tissue, resulting in the power being wasted. On the other hand, if the bandwidth is low, the created image does not have a good resolution, creating problems. First, we do not understand the tumor's location, and second, if the tumor is close to a larger object, such as a sizeable mammary gland, we no longer perceive its existence. So it is essential to know how much bandwidth the signal is sending. In addition, some frequencies may not be suitable within this bandwidth. For example, the body passes the frequency of 1 to 2GHz well, absorbs 2 to 2.5GHz and then passes 2.5 to 5GHz well. In this case, we should not send a signal with frequencies 2 to 2.5GHz because all of it is absorbed and therefore is of no use.

The FCC has authorised a frequency range between 3.1GHz and 10GHz for ultra-wideband medical imaging devices [17]. As a result, our sensor was designed to fall within this range. The simulation process was generated by CADFEKO 2018 with the design consisting of hemispherical breast tissue with a diameter of 5.4cm and two dipole antennas with a length of 5.5cm, one of which transmits a signal and the other which receives it. Dipole antennas are chosen for design due to their low production cost and simplicity where the phantom devoid of tumor is placed between the antennas, as depicted in Fig. 1.

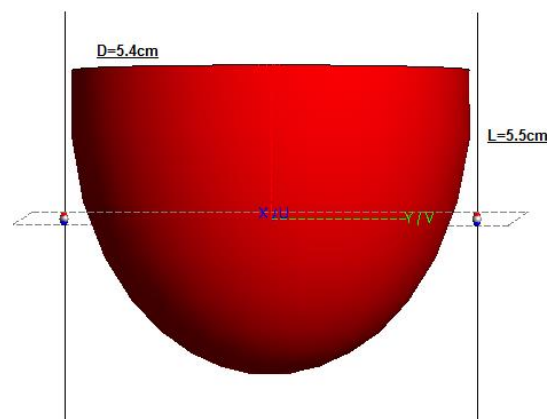


Figure.1. 3D breast model without an embedded tumor.

The phantom of breast size remained the same in the second design, but an intra-breast tumor was added. As shown in Fig. 2, the spherical tumor had a 5mm radius. Due to this specific tumor size, breast cancer can be effectively treated if detected as early as 1-10mm.

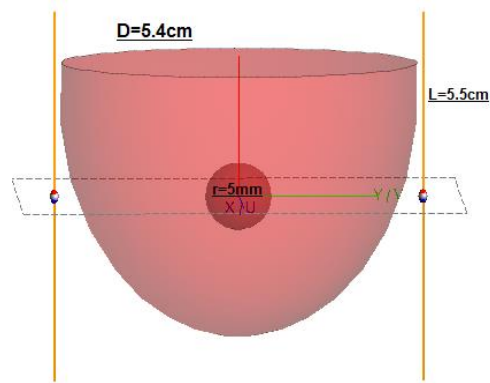


Figure 2. 3D breast model with tumor embedded.

The tumor's location to see its effect on the results of the reflection coefficient and the transmission coefficient; in the first case, the tumor was placed near the transmitter antenna, as shown in Fig. 3.

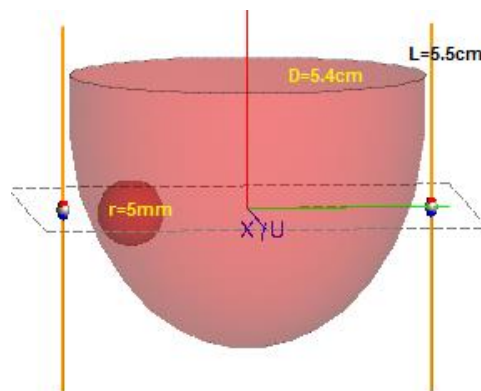


Figure 3. 3D breast model with a tumor embedded near the transmitter.

In the other case, we changed the tumor location near the second antenna representing the receiver antenna, as shown in Fig. 4, to compare the reflection and transmission coefficient results between this case and the previous case.

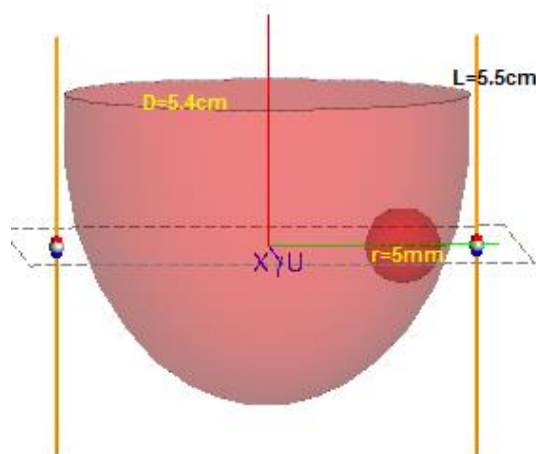


Figure 4. 3D breast model with a tumor embedded near the receiver.

4. Simulation and Results

The input and output relationship between antenna ports was described by S-parameters, also known as reflection coefficients. The reflection coefficients that the device attempts to deliver to the antenna are denoted by S11. To obtain the measured S11, the phantom with no tumor between the two antennas was simulated, as shown in Figure 5.

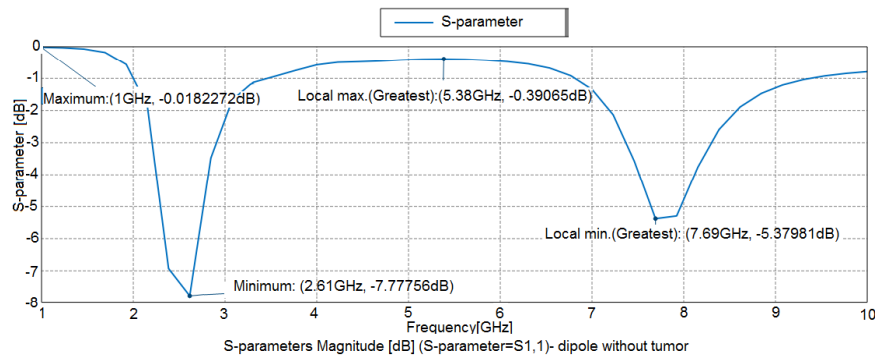


Figure 5, S11 in the breast phantom model without tumor.

Fig. 6 shows that the reflection coefficient increases marginally with the presence of the tumor in our breast phantom model.

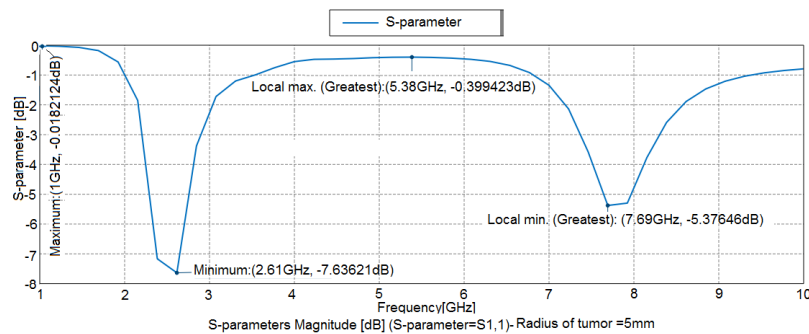


Figure. 6. S11 in the breast phantom model with tumor r=5mm.

When the transmission coefficient S_{12} , which represents power transferred from port 2 to port 1 was simulated, the following results were obtained, which show that there is a clear difference in the results of the breast condition with the presence and the absence of the tumor as shown in Fig. 7.

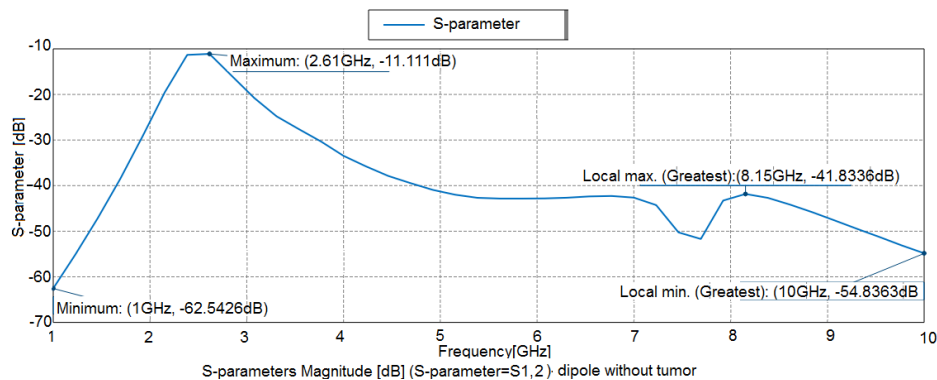


Figure 7. S12 in the breast phantom model without tumor.

Figure 8 shows that the transmission coefficient increases with the presence of the tumor in our breast phantom model.

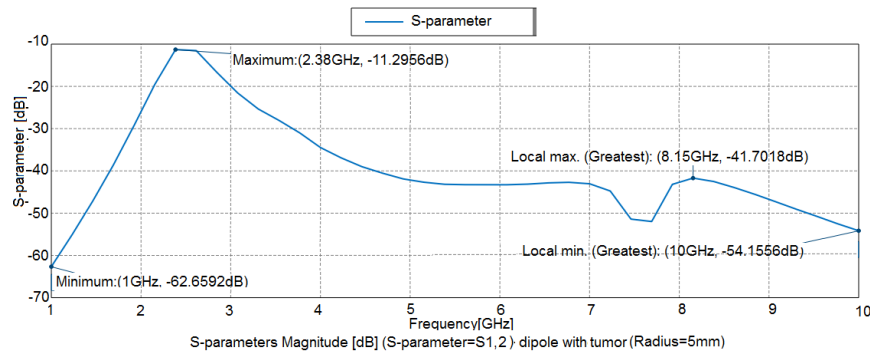


Figure 8. S12 in the breast phantom model with tumor.

This simulation aims in order to see how tumors affect the reflection coefficient S11 and transmission coefficient S12 at the frequency range and then look for a clue in the S-parameters to build breast images without background data. After performing the simulation, it was found that there would be a noticeable change in the results when the tumor was placed near the transmitter, as shown in Fig. 9.

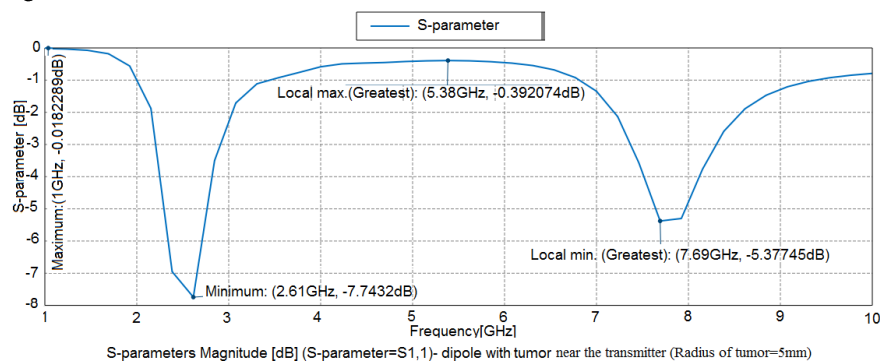


Figure 9. S11 in the breast phantom model with a tumor near the transmitter.

When the tumor was placed near the transmitter (the new values of the transmission coefficient S12), there would also be a noticeable change in the results, as shown in Fig. 10.

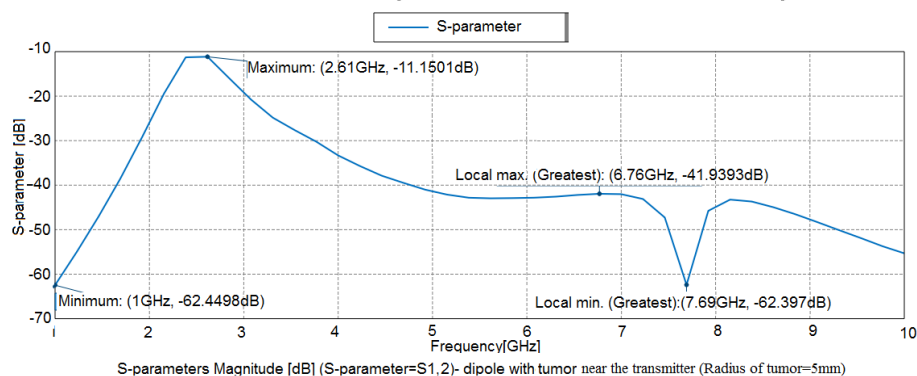


Figure 10. S12 in the breast phantom model with a tumor near the transmitter.

When the simulations for the second case; it was found that when the tumor was placed near the receiver, there would be a noticeable change in the results where the reflection S-modulus of S11, as shown in Fig. 11.

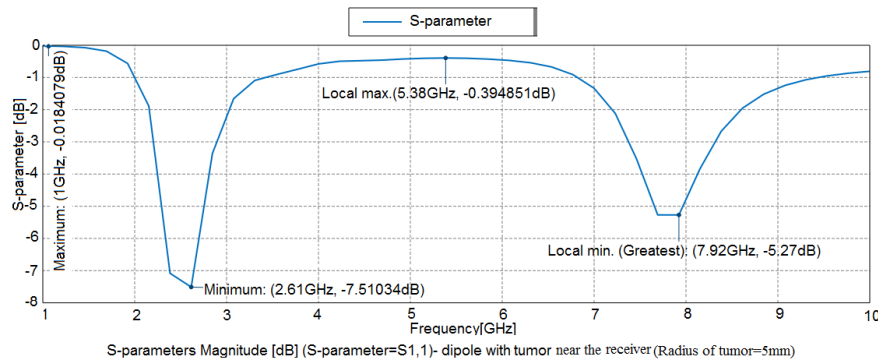


Figure 11. S11 in the breast phantom model with a tumor near the receiver.

While the new values of the transmission coefficient S12 in the case when the tumor was placed near the receiver, there would be a noticeable change in the results, as shown in Fig. 12.

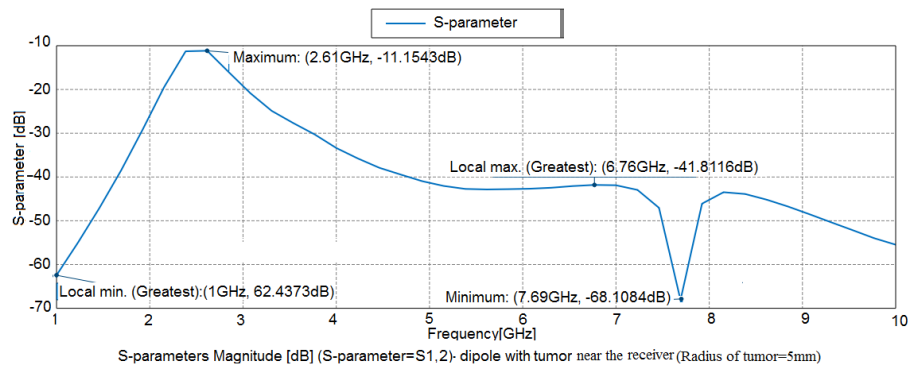


Figure 12. S12 in the breast phantom model with a tumor near the receiver.

The tumor's dielectric coefficient (conductivity and permittivity) was gradually changed until the value will be close to the dielectric coefficient of breast tissue. In each case, simulations were run in order to find out the results obtained and the difference between cases in the results of the transmission coefficient and the reflection coefficient when the dielectric coefficient is gradually changed. Table 1 shows the tumor's dielectric coefficient (conductivity and permittivity) with frequencies from 0.5GHz to 10GHz.

Table 1. The dielectric coefficient of the tumor before any change in the parameters.

Frequency (GHz)	Relative permittivity	Conductivity
0.5	66.696	1.697
2	63.008	4.164
4	59.125	6.774
6	56.551	8.487
8	55.425	9.242
10	53.630	10.112

In the first case, we also changed the tumor parameters (permittivity and conductivity) to approach the parameters of dielectric of the breast tissue, as shown in table 2.

Table 2. The dielectric coefficient of the tumor for the first change.

Frequency (GHz)	Relative permittivity	Conductivity
0.5	21	0.187
2	19	0.436
4	17	0.78
6	15	1.25
8	13	1.7
10	11	2.1

Fig. 13 shows the change in the results of the reflection coefficient when compared with the results of the original parameter value, where the reflection S-parameter S11 was measured.

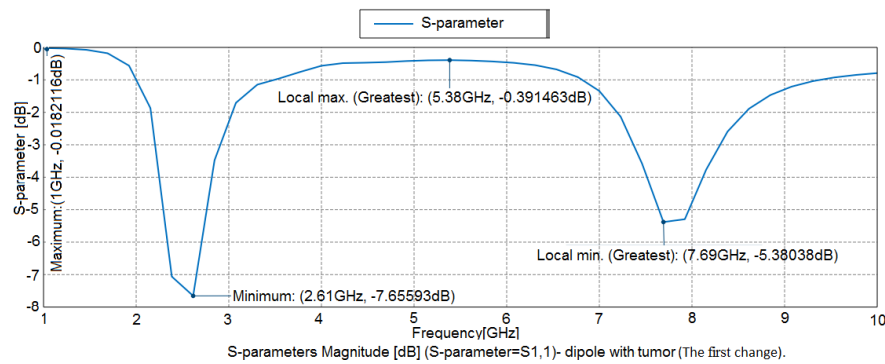


Figure 13. S11 in the breast phantom model with the tumor for the first change.

Also, when we simulated the transmission coefficient S12, we obtained the following results below, which show a very slight change in the results, as shown in Fig. 14.

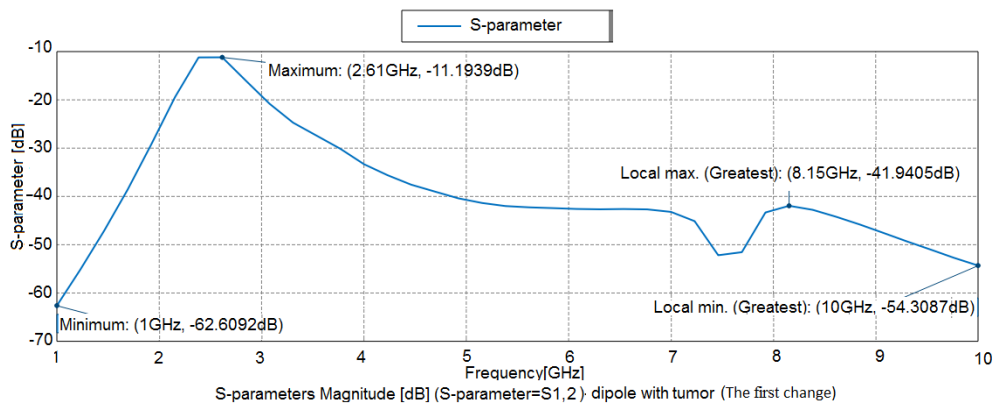


Figure 14. S12 in the breast phantom model with the tumor for the first change.

5. Discussion

A closer examination of the curves in Figures 5 and 6 reveals that the curve goes slightly upward compared to the one without the tumor, indicating that the tumor's presence influences the results.

When the transmission coefficient S_{12} from port 2 to port 1 was simulated, there was a clear difference in the results of the breast condition with the presence and the absence of the tumor.

When the simulations for the second case were run, it was found that when the tumor was placed near the receiver, there would be a noticeable change in the results where the reflection S-modulus of S_{11} .

After the simulation, it was found that when changing the parameters of the dielectric of the tumor, there would be a slight change in the results of the reflection coefficient when compared with the results of the original parameter value.

A very slight change in the results was obtained, when the transmission coefficient S_{12} was simulated.

6. Conclusion

The tumor was diagnosed based on the difference in conductivity and permittivity between cancerous and healthy breast tissue. The results and simulation resulting from the designs showed a difference between the breast design results containing a tumor and the design results that do not have a tumor. Simulation results revealed a distinction between results (S_{11} and S_{12}) depending on whether the tumor is located close to the transmitter or receiver antenna. Finally, the results (S_{11} , S_{12}) demonstrated a distinct difference when the tumour's dielectric coefficient (conductivity and permittivity) is altered gradually until it approaches the dielectric coefficient value of breast tissue. Therefore, the simulation's results and signals can be analysed to determine if a tumor exists. This paper shows an apparent change in the global maximum, minimum, second maximum, and minimum values for each transmission coefficient and reflection coefficient.

References

- [1] American Cancer Society. Key Statistics for Breast Cancer. 2022, ; Available from: <https://www.cancer.org/cancer/breast-cancer/about/how-common-is-breast-cancer.html>.
- [2] Berger, F., et al., Randomised, open-label, multicentric phase III trial to evaluate the safety and efficacy of palbociclib in combination with endocrine therapy, guided by ESR1 mutation monitoring in oestrogen receptor-positive, HER2-negative metastatic breast cancer patients: study design of PADA-1. 2022. 12(3): p. e055821.in 2022 BMJ open.
- [3] Wassila, S., M. Lotfi, and M.S. Mohammed. Breast cancer Detection Using the SVR Approach For Different Configurations of Microwave Imaging System. in 2019 6th International Conference on Image and Signal Processing and their Applications (ISPA). 2019. IEEE.
- [4] Kwon, S. and S.J.I.j.o.b.i. Lee, Recent advances in microwave imaging for breast cancer detection. in 2016 International journal of biomedical imaging.
- [5] Gabriel, S., et al., The dielectric properties of biological tissues: III. Parametric models for the dielectric spectrum of tissues. in 1996 Physics in medicine & biology. 41(11): p. 2271.
- [6] Wang, Z., et al., Medical applications of microwave imaging. in 2014 The Scientific World Journal.

- [7] Koch, D.K., Dual Source Excitation Rectangular Waveguide Design and Evaluation for the Measurement of Electromagnetic Material Properties. 2018.
- [8] Fontaine, G., Initial design and simulation of a portable breast microwave detection device. 2022, University of manitoba.
- [9] Vemulapalli, S., Early Breast Cancer Diagnosis Using Microwave Imaging via Space-Frequency Algorithm. 2017, University of Missouri--Kansas City.
- [10] Vemulapalli, S., M. Khan, and D. Chatterjee. Analysis of ultrawideband microwave imaging via space time beamforming algorithm in the frequency domain. in 2015 IEEE Applied Electromagnetics Conference (AEMC). 2015. IEEE.
- [11] O'Halloran, M., et al., Anatomy and Dielectric Properties of the Breast and Breast Cancer, in An Introduction to Microwave Imaging for Breast Cancer Detection. 2016, Springer. p. 5-16.
- [12] Priyadarshinee, S., et al., Studies of structural, microstructural, optical and dielectric properties of GdMnO₃. 2022: p. 1-12.
- [13] Lazebnik, M., et al., A large-scale study of the ultrawideband microwave dielectric properties of normal breast tissue obtained from reduction surgeries. in 2007 Physics in medicine. 52(10): p. 2637.
- [14] Matković, A., et al., Complex Permittivity of Ex-Vivo Human, Bovine and Porcine Brain Tissues in the Microwave Frequency Range. in 2022 Diagnostics. 12(11): p. 2580.
- [15] Yildiz, G., et al., Antenna Excitation Optimization with Deep Learning for Microwave Breast Cancer Hyperthermia. in 2022 Sensors. 22(17): p. 6343.
- [16] Xie, Z., A Microstrip Antenna for Medical Application: Tissues Detection. 2017.
- [17] Foster, K.R. and J.L. Schepps, Dielectric Properties of Tumor and Normal Tissues at Radio through Microwave Frequencies. Journal of Microwave Power, 1981. 16(2): p. 107-119.